

Back-iron Extension Thermal Benefits for Electrical Machines with Concentrated Windings

Fengyu Zhang, David Gerada, Zeyuan Xu, Xiaochen Zhang, Chris Tighe, He Zhang and Chris Gerada



**University of
Nottingham**

UK | CHINA | MALAYSIA

Faculty of Science and Engineering, University of Nottingham Ningbo
China, 199 Taikang East Road, Ningbo, 315100, Zhejiang, China.

First published 2019

This work is made available under the terms of the Creative Commons
Attribution 4.0 International License:

<http://creativecommons.org/licenses/by/4.0>

The work is licenced to the University of Nottingham Ningbo China
under the Global University Publication Licence:

<https://www.nottingham.edu.cn/en/library/documents/research-support/global-university-publications-licence.pdf>



**University of
Nottingham**

UK | CHINA | MALAYSIA

Back-iron Extension Thermal Benefits for Electrical Machines with Concentrated Windings

Fengyu Zhang, David Gerada, Zeyuan Xu, Xiaochen Zhang, *Member, IEEE*, Chris Tighe, He Zhang, *Senior Member, IEEE* and Chris Gerada, *Senior Member, IEEE*

Abstract— This paper proposes a novel, low-cost, effective way to improve the thermal performance of electrical machines by extending a part of the back-iron into the slot. This modification helps in reducing the thermal resistance path from the center of the slot to the coolant, however its thermal benefits must be clearly evaluated in conjunction with the electromagnetic aspects, due to the higher iron losses and flux-leakage, and furthermore such an extension occupies space which would otherwise be allocated to the copper itself. Taking a case study involving an existing 75kW electric vehicle (EV) traction motor, the tradeoffs involving the losses, flux-leakage, output torque, torque-quality and the peak winding temperature with back-iron extension (BIE) and without are compared. Finally, experimental segments of the aforesaid motor are tested, verifying a significant 26.7% peak winding temperature reduction for the same output power with the proposed modification.

Index Terms—Thermal management, machine cooling, power density, thermal analysis, thermal resistance network, slot cooling

I. INTRODUCTION

WITH the increasingly stringent emissions legislations, there is an unprecedented demand for transport electrification, be it for rail, marine, aerospace or automotive. For some applications this involves hybridization of the conventional engine-based systems, while for other applications all-electric architectures are developed [1, 2]. The core component in these electrified architectures is the electrical machine, and hence its performance improvement merits detailed research in order to achieve important

performance metrics such as high efficiency, high power density (kW/kg, or kW/L), and equally important a low cost (\$/kW) in order to make a strong business case and increase market proliferation [3]. While material developments are an enabler for improved performance, often new materials come with an increased cost premium. It has been shown that improvements in thermal management are a key enabler to push machines' technological boundaries [2].

Automotive and railway traction machines are required to specifically have a high torque density, low inertia, wide constant power -speed ranges and high reliability as demanded by the market. Various ambitious cost and performance targets have been set by related governmental bodies, such as the Department of Energy (DoE) in the USA, which has set the FreedomCar 2020 targets, and the Advanced Propulsion Centre (APC) in the UK [4]. The maximum allowable temperature in an electrical machine's stator is typically determined by the constituent insulation materials' thermal limit pertaining to the windings, with various industrial classes of insulation set, such as class H (180 °C) and class C (220 °C). Thus improved cooling enables higher power densities in electrical machines, which helps to reduce weight, volume and cost. Improved thermal management pushes winding current density higher before reaching the maximum winding temperature limit, which is one critical factor determining the motor torque production [5]. Reducing losses generated in the machine is of course another alternative way from heat sources view to improve the thermal condition of the motor. In the ideal case, the two methodologies of cooling improvement and losses reduction are coupled, in order to find the optimum tradeoff between the two in light of the specific optimization targets.

For higher power density machines, using water or oil as a cooling medium, yields better thermal performance with respect to the air-cooled machines. CFD and experimental results indicate that wet stator cooling [6, 7] leads to markedly better thermal conditions compared to the indirect cooling methods and the traditional water-jacket cooling [8]. In [9] the thermal performance of a machine with both the stator and rotor flushed directly by coolant is investigated. However, with either the wet stator or totally wet cooling method, lots of accessory components have to be mounted, which increase the system complexity and reduce reliability. Also having stator and rotor wet cooling adds extra rotational friction losses and is thus only suitable for very specific circumstances such as in

Manuscript received November 9, 2018; revised January 6, 2019; accepted February 19, 2019. This work was supported by China NSFC under Grant 51607099 and by the Ningbo Science & Technology Beauru under Grant 2017D10029.

F. Zhang, D. Gerada, H. Zhang (corresponding author), and C. Gerada are with the Power Electronics, Machines and Control group, University of Nottingham Ningbo China, Ningbo 315100, China (e-mail: fengyu.zhang@nottingham.edu.cn; David.Gerada@nottingham.ac.uk; he.zhang@nottingham.edu.cn; Chris.Gerada@nottingham.edu.cn).

D. Gerada, Z. Xu, X. Zhang and C. Gerada are with University of Nottingham, NG7 2RD, UK (e-mail: David.Gerada@nottingham.ac.uk; Zeyuan.Xu@nottingham.ac.uk; Xiaochen.Zhang@nottingham.ac.uk; Chris.Gerada@nottingham.ac.uk).

C. Tighe is with Electrical Cooling Solutions Ltd, UK (email: chris.tighe@electricalcoolingsolutions.com).

the case of lower speed machines. Therefore, in industrial machines (for example those used in automotive traction), the external cooling jacket is widely adopted as a robust cooling methodology.

Often, one major bottleneck in the thermal improvement of motors with indirect cooling is the equivalent thermal conductivity perpendicular to the winding orientation in the slot which is poor due to the multiple layers of insulation involved (typically the insulation build up consists of wire enamel, slot impregnation resin, air-pockets, and the slot liner) [10, 11]. In light of this some novel cooling methods targeting directly the heat directly inside the slot have been proposed. As described in [12-17], slot water jacket cooling provides an efficient way to reduce the winding hot spot temperature, albeit the copper losses are increased due to the space occupied by the slot jacket. Moreover due to electrical conductivity of water, it is imperative that sealing is ensured within such a configuration. A novel heat path has been proposed and experimentally validated in [5], where a piece of thermally conductive material is inserted into the slot of a low frequency machine, benefiting approximately from a 40% hot-spot temperature reduction for the same current loading. However, this method adds extra eddy current losses, which might nullify the effect the heat path brings, especially with higher frequency machines as in the case of automotive traction. In [18], the authors study the effects of different winding design on the motor loss distribution and the balancing effects between stator iron loss and rotor loss.

Electromagnetic and thermal aspects are closely coupled and interlinked in the machine design process, which makes it irrelevant to modify the motor geometry from the thermal point of view only. For thermal engineers, it is thus critical to ensure that the benefit in any proposed novel thermal technique is not outweighed by the deterioration in other aspects such as the torque (and its quality), or the machine losses. In [19], flux-barriers are inserted in the stator lamination and simulation results are compared to the more conventional indirect water cooling jacket, with benefits of 10% temperature reduction in the slot region of the machine observed. However, the aforementioned arrangement needs extra pump power and sealing due to possible water leakage. The effects of parallel and trapezoidal slot shapes on the loss distribution and the heat transfer characteristics are compared and researched in [20]. It is concluded that parallel slots are more advantageous, with a 35% improvement in the heat transfer path between the slot and the stator core pack noted, which yields a net 8% improvement in the output per active weight capability of the machine. The benefits noted however can only be achieved with open-slot modular stator windings.

This paper proposes and experimentally verifies a novel way to decrease the equivalent thermal resistance between the hot spot and the coolant by extending a small part of back-iron into the middle of the slot, where the hot spot is located. This paper is organized as follows: Section II introduces the principle behind the back-iron extension (BIE) and discusses multi-domain models and considerations involved in optimizing the geometry of the back-iron extension. The

results of the optimization are experimentally verified and further discussed in Section III. Finally the conclusions of this research are summarized in Section IV.

II. BACK-IRON EXTENSION

As mentioned in the introduction, this paper proposes a part of the back-iron extended from the middle point of the slot bottom along the centreline of the slot to the slot opening, as shown in Fig. 1. In water-jacket cooled machines, most of the heat generated in the slot is dissipated to the stator lamination, through the slot wall, to the stator tooth, or directly to the stator back-iron, and then to the jacket coolant. Back-iron extension provides another alternative heat transfer path for heat to be removed to the back-iron, increasing the contact area between the slot and stator lamination, and shortening the equivalent thermal resistance between the hot spot in the slot and coolant, which is typically located in the middle of the slot.

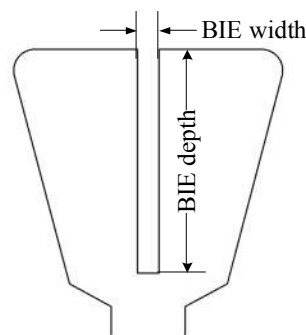


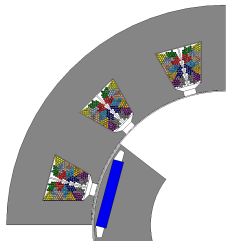
Fig. 1. Back-iron extension geometry

This section analyses the thermal benefits of the back-iron extension, taking as a case study an existing 75kW 12slot, 8-pole Permanent Magnet machine, with concentrated winding used for an electric vehicle shown in Fig. 2 and the relevant data listed in Table 1. The electromagnetic effects of the back-iron extension are also considered, due to the flux leakage through back-iron extension and additional iron-losses generated within. The optimized back-iron extension geometry is generated based on the rated power of the traction machine under investigation, with guidelines given about the optimized BIE geometry on machines of different size.



Fig. 2. Traction machine

TABLE I
 TRACTION MACHINE PARAMETERS

Machine type	Three – phase PMSM		
Machine Rating:			
Voltage	384 V	480 V	
Rated/ peak power	37/74 kW		
Rated/ peak torque	126/382 N.m		
Maximum speed	10000 rpm		
Working time at peak power	≥60 s	Working temperature	-40 ~ 105°C
Efficiency	≥95%	Coolant:	Ethylene water glycol – EWG 50/50
Geometry:		Materials:	
Outer diameter	245 mm	Magnet	N38EH
Active length	140 mm	Iron sheets	M235 – 35 A
		Winding	copper

A. Thermal modelling of BIE

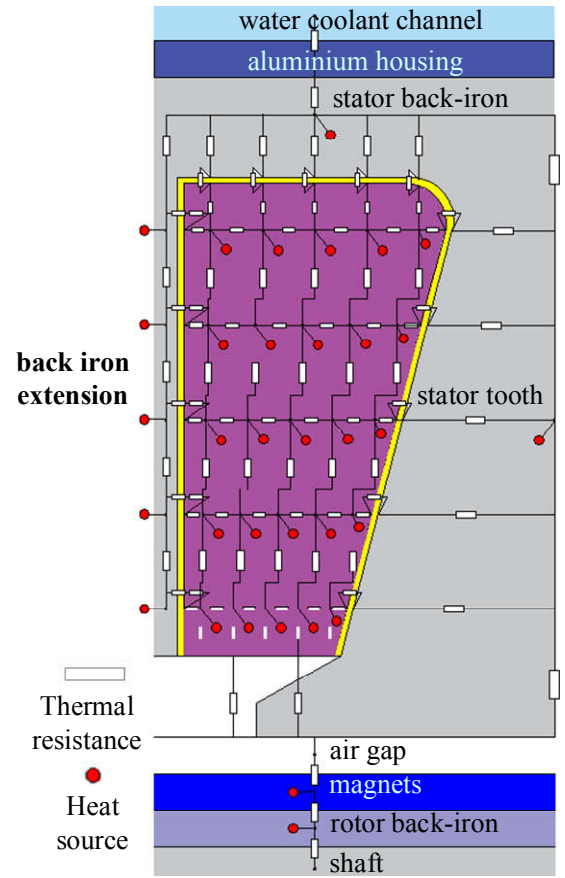
Lumped Parameter Thermal Network (LPTN), is a widely used tool in electrical machine thermal analysis which provides quick answers for cooling parametrized studies for a selected cooling methodologies. A LPTN thermal model is developed to investigate the thermal performances of the BIE cooling concept for the machine described in previous section.

Heat transfer paths in both the radial and axial directions are simulated in the 3D thermal model, with three longitudinally divided parts in the machine core and one part for each end-winding. The longitudinal lengths of the core machine parts are 20 mm, 100 mm, and 20 mm, adding up to the net 140mm active length detailed in Table I. Exploiting symmetry 1/24th of the stator and 1/16th of the rotor are simulated. The half slot includes 25 nodes, with a 5×5 distribution to achieve a detailed temperature distribution. Fig. 3 (a) shows the radial thermal network of the motor with BIE in the center of the slot and (b) displays the corresponding axial thermal network, where the 25 nodes in the slot in (a) are not shown on purpose to give a clear view of the heat flow longitudinally.

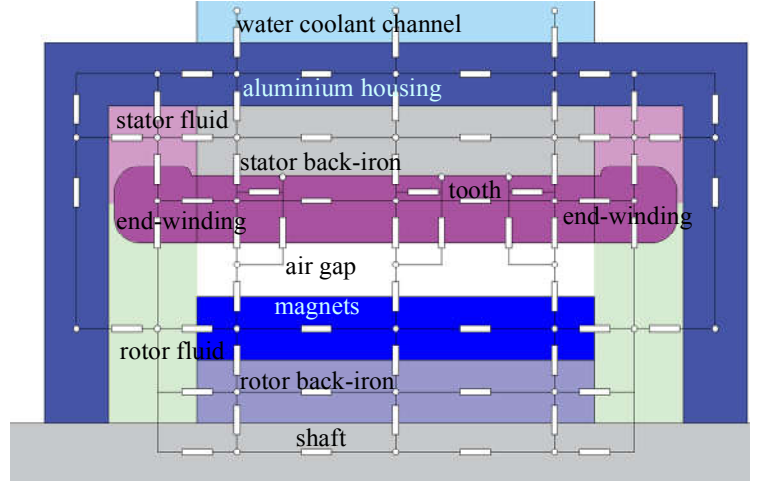
Heat losses from the water jacket of the traction machine to ambient air are neglected, as they are very small compared to the heat transfer to the coolant. An isothermal boundary condition is applied to the coolant based on an assumption that the water jacket is sufficiently effective to remove all the heat generated. The two sides where the BIE and stator tooth are connected to other parts in Fig. 3 (a) are assumed adiabatic due to the geometrical symmetry.

A heat conservative equation for any node and all its neighboring nodes, shown in Fig. 3, can be expressed by the following (1):

$$q_i + \sum_{j \neq i}^n \frac{T_j - T_i}{R_{ij}} = 0 \quad (1)$$



(a)



(b)

Fig. 3. Thermal network of developed motor with back-iron extension

where node j is an adjacent node to node i in the thermal network, q_i is the loss generated in node i ; T_i , T_j are the temperatures in node i and node j respectively, while R_{ij} is the thermal resistance between node i and node j .

The losses considered in the modelling are I^2R copper losses, stator iron losses, rotor iron losses and magnet losses. All losses are assumed uniformly generated in the corresponding parts of the machine, added to the nodes as a heat source, respectively. Transient temperature analysis can be determined by adding thermal mass to each node.

Only conduction heat transfer and convection heat transfer are included in the LPTN thermal model. The thermal resistances by conduction between neighboring nodes applied in (1) can be determined from [21-23]:

$$R = l/\lambda A_{cross} \quad (2)$$

where l is the distance between the nodes along the heat flow, A_{cross} is the cross-sectional area (perpendicular to the heat flow), and λ is the thermal conductivity of the node material. Different values of thermal conductivity are applied to the radial and axial directions of the winding in the slot, stator and rotor iron. Effective thermal conductivity λ_{cu} is used in calculating the thermal conductivity of the winding in the slot [11], taking into account the various constituent materials. Equation (2) is the classic equation for conductive thermal resistance. An alternative method is presented in [24, 25] to calculate the thermal conductive resistance, which suggests a more accurate temperature distribution considering internal heat generations, such as copper and iron losses.

Convective heat transfer occurs primarily in three places where fluid flows over the machine solid parts: (i) between coolant and housing, (ii) the air-gap between rotor and stator core, and (iii) machine end region where end-winding is directly cooled by air in the region. For convection, the thermal resistance in (1) is calculated from (3):

$$R = 1/hA_{sur} \quad (3)$$

where A_{sur} is the surface area of solid to the fluids and h is the heat transfer coefficient and can be calculated as follows.

The flow inside the water cooling jacket is considered turbulent. The heat transfer coefficient between the coolant and aluminum housing applied in (3) can be calculated by (4) to (6) [26]:

$$N_u = \frac{(f/8) \times (R_e - 1000) \times P_r}{\left[1 + 12.7 \times (f/8)^{0.5} \times (P_r^{2/3} - 1)\right]} \quad (4)$$

$$h = \lambda N_u / D_h; \quad R_e = \rho v D_h / \mu; \quad D_h = 4S/P \quad (5)$$

$$f = (0.79 \times \ln(R_e) - 1.64)^{-2} \quad (6)$$

where f is friction factor, λ is the thermal conductivity of the fluid (water), R_e is the Reynolds number, P_r is the coolant Prandtl number, D_h is the hydraulic diameter, v is the water velocity, and μ is the dynamic viscosity of water. In the above equations S and P are the cross section area and peripheral length of the water channel respectively.

The air flow across the air-gap is calculated from (7) to (8) [21]:

$$h = 0.386 \lambda T_a^{0.5} P_r^{0.27} / D_h \quad (7)$$

$$T_a = R_e \sqrt{l_g / R_r}; \quad R_e = \rho v l_g / \mu; \quad D_h = 2l \quad (8)$$

where λ is the thermal conductivity of the air, T_a is the Taylor number, P_r is air Prandtl number, D_h is the hydraulic diameter, R_e is the Reynolds number, l is air-gap length, R_r is the rotor radius, ρ is the air density, v is the air velocity, and μ is the dynamic viscosity of air.

In order to calculate the heat transfer coefficient between the end-winding and stator/rotor fluid in (b), equation (9) is used [21]:

$$A = k_1 \times (1 + k_2(v)^{k_3}) \quad (9)$$

where v is the rotor velocity while k_1 , k_2 and k_3 are curve fitting coefficients. In the thermal network, $k_1=15$,

$k_2=0.15, k_3=1$.

In this paper, both the width and depth of the back-iron extension are optimized to provide the best cooling benefits. The back-iron extension width ranges from 0 to 4 mm, while the BIE depth is varied from 0 to the entire slot depth of 21.7mm, as described by Table 2. The introduction of BIE, reduces the slot area available for winding (winding area), resulting in a decreased copper fill factor as shown in Fig. 4. It is worth noting that in this paper, the ‘copper fill factor’ in Fig. 4, is defined as the ratio of copper area for each motor with the proposed BIE divided by the original motor slot area, maintaining the same ratio of copper area to the available winding area. The available winding area reduces with the introduction of the BIE, hence the amount of copper in the slot reduces with respect to the original design without the BIE.

The thermal resistance formulas used with the circuit of the original motor are similar to those used with the motor using BIE, which are based on node geometry and material thermal conductivity, except for the resistances on the added heat transfer path(i.e. BIE). The loss sources are also different for the two thermal models, as will be discussed in more detail in the subsequent section.

TABLE 2
BACK-IRON EXTENSION GEOMETRY VARIATIONS

Simulation	Back-iron Extension Depth	Back-iron Extension Width
	mm	
BIED1	4.34 (1/5 of slot depth)	0.1 – 4 (0.1 mm) interval gap
BIED2	8.48 (2/5 of slot depth)	
BIED3	10.32 (3/5 of slot depth)	
BIED4	17.36 (4/5 of slot depth)	
BIED5	21.7 (full slot depth)	

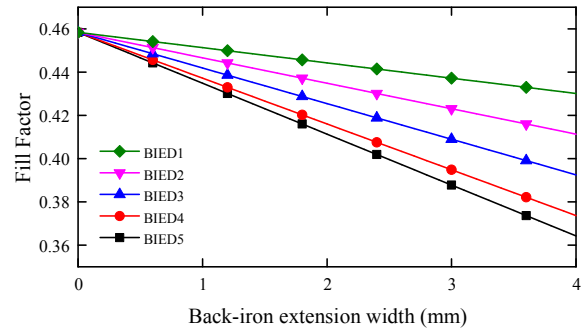


Fig. 4. Copper fill factor with BIE geometry variations

B. Electromagnetic aspects of back-iron extension

Finite Element Analysis (FEA) is used to analyze the non-linear electromagnetic effects and to combine with the thermal model of the previous section so that any geometric change can be instantly assessed from both the electromagnetic and the thermal domains. It is worth noting that adequate mesh refinement is conducted in the back-iron extension. The introduction of the BIE causes additional flux leakage through the extension, especially when the back-iron extension depth is large which in turn reduces the output torque of the motor. Fig. 5 shows the flux density contour for the same BIE dimension drawn in Fig. 3(a). Because of the additional flux leakage introduced by the BIE, higher current will be demanded to generate the same output torque, resulting in

increased copper losses generated in the slot and higher iron loss generated in the stator core itself. Furthermore, additional iron losses are generated within the BIE itself.

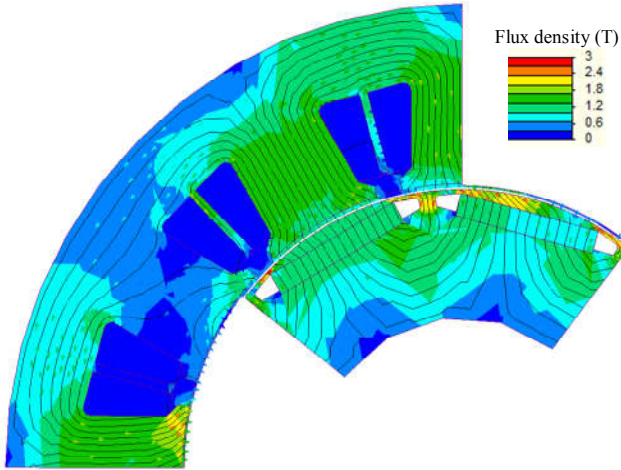


Fig. 5. Flux density contour at rated torque with BIE

Considering BIE depth and width variations, analysis is conducted with an input current of 90A (this current corresponding to the rated current of the original motor) firstly and output torque is calculated, as shown in Fig. 6 (a). In this figure, the different BIE depths (BIED 1-5) corresponding to Table 2 are represented by the different lines, while for each depth, different BIE widths are considered on the x-axis. When the BIE depth is small (under 8.48mm), the output torque is not really affected no matter how wide the back-iron extension is. This is within expectation, as it is difficult for flux leakage to be significant with a shallow back-iron extension as verified by Fig. 6 (b), which plots the maximum flux density in the air-gap corresponding to the lines in Fig. 6 (a) for a BIE width of 4mm. The maximum flux density in the air-gap of the BIE motor is almost same with that in the original motor when the output torque is not affected by the BIE introduction. On the other hand, with BIE depths beyond 10.32mm (BIED4, BIED5), the maximum flux density decreases and torque starts to show a reducing tendency and drops by up to 1.59 % from 107.3Nm down to 105.6Nm when the back-iron extension width is 4 mm, and the depth is equal to the slot height (i.e. BIED5).

Fig. 6 (c) shows the required increase in current (beyond the original 90A) to keep the output torque constant as with the original machine. The maximum increase in current is 2.17 % when the torque drops to its lowest value of 105.6 Nm.

Torque quality is also another important aspect which needs assessment when proposing such a geometrical modification. Fig. 7 shows the increase in torque ripple for various BIE geometries with a maximum increase in torque ripple of up to 10% for the same output torque.

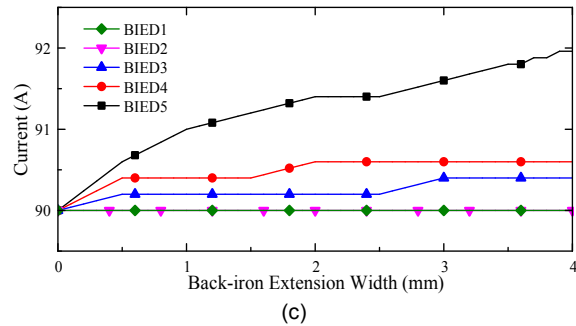
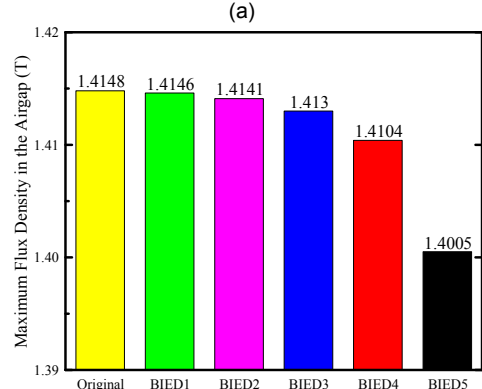
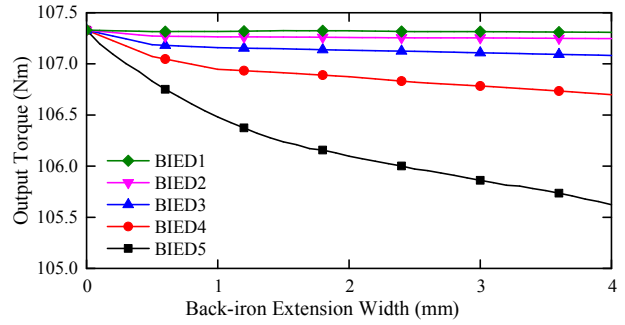


Fig. 6. (a) Output torque reduction with back-iron extension, (b) maximum air-gap flux density with back-iron extension and (c) required current increase to maintain the same output torque

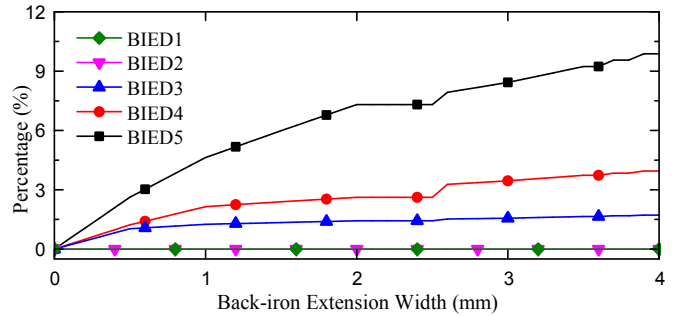


Fig. 7. Torque ripple increase for various BIE geometries

To maintain the same output torque, the effect of current requirement increase on the thermal performance of the machine reflects in both the loss magnitude as well as the loss distribution. Higher current increases the flux density within the stator core due to the stronger armature field, and hence the iron losses therein increase. Furthermore, additional iron losses are generated within the back iron extension itself. The copper I²R losses increase as well, both due to the aforesaid

increased current requirement, as well as due to the increased resistance since the BIE occupies space which would otherwise be available for copper. Therefore, with increased BIE width at constant BIE depth, copper losses I^2R increase due to increased electrical resistance resulting from the reduced copper fill factor, within periods when current remains same in Fig. 6 (c). Fig. 8 summarizes the increase in stator iron losses (which also include iron losses generated within the BIE itself), and copper losses with respect to the original design. For the copper losses (P_{cu}) the loss increase is up to 26%, while the iron losses (P_{Fe}) increase by up to nearly 9%.

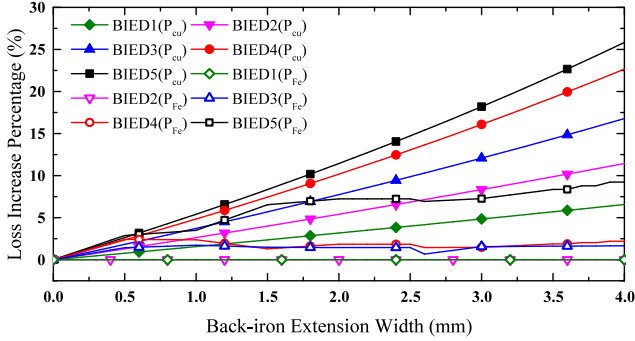


Fig. 8. Loss increase with back-iron extension

C. Thermal benefits of back-iron extension

From the foregoing discussions it is clear that the selection of the BIE geometry is a multiphysics problem since on one side the thermal path for the losses is improved, but on the other hand, the additional copper and iron losses can increase significantly.

The balance between these two aspects determines whether BIE brings about any thermal benefits to the motor. Combining the thermal tool of section A with the analysis of section B in a single iterative design environment, where thermal conductivities (and losses) are adjusted with temperature until a defined convergence is achieved, Fig. 9 is obtained. In Fig. 9 (a) the peak winding temperature at the rated torque is shown for the full sweep of BIE geometries considered, with the line at 173°C representing the peak temperature for the original machine. Fig. 9 (b) shows the net peak temperature difference as a percentage (%) with respect to the original machine.

For the case of a very short BIE (BIED1), the increased losses outweigh the thermal benefit. Thermal improvements are observed for BIED2 and BIED3, especially when the BIE width is small, with winding temperature reductions of up to 3% and 8% respectively. For deeper back iron extensions, BIED4 and BIED5, representing radial BIE projections of 80% and full slot depth, the reduced slot thermal resistance is in largely dominant over the increasing losses and improved thermal performance is observed for all the investigated BIE widths. Peak winding temperature reductions of up to 14% and 19.3% are observed when the BIE width is around 1.6 mm and 2.2mm respectively. It is worth noting that peak winding temperature is more sensitive to BIE width value up to 0.7 mm, with the peak winding temperature dropping by down to 8 °C in this region. When BIE width increases beyond the

forementioned values no significant temperature reduction is observed. Table 3 summarizes the optimized BIE width for the different BIED considered, together with the corresponding peak winding temperature reduction.

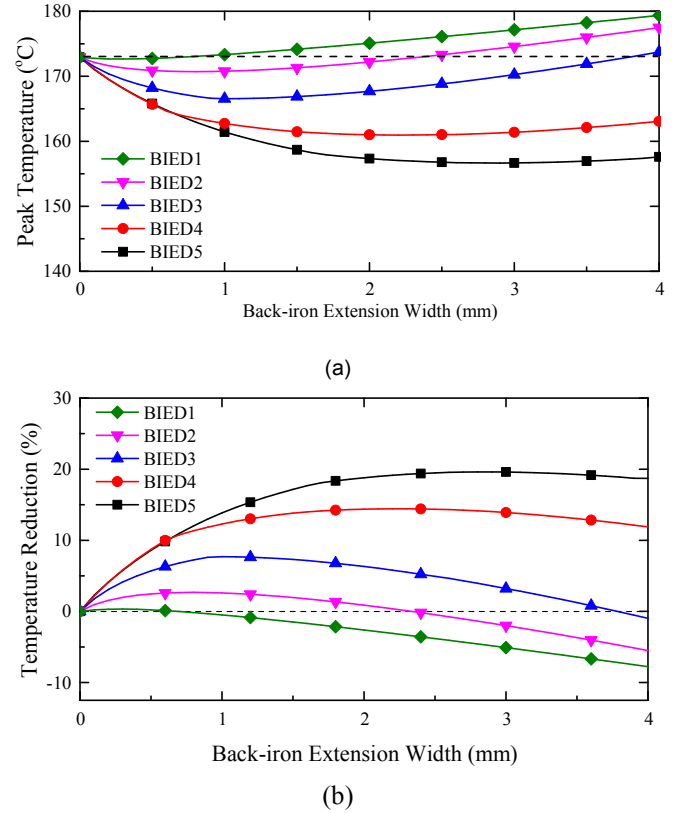


Fig. 9 (a) Peak winding temperature (b) Peak winding temperature variation with BIE dimensions for rated torque condition

TABLE 3
OPTIMIZED BIE WIDTH AND IMPROVED WINDING TEMPERATURE

Simulations	Optimized BIE width	Temperature reduction	Winding temperature reduction percentage
	mm	°C	%
BIED2	0.7	2.28	2.68
BIED3	1	6.45	8
BIED4	2	12	14
BIED5	2.2	16	19.3

The BIE reduces the peak winding temperature mainly by shortening the heat transfer path between the hot spot in the slot and the coolant. The temperature distributions of half the slot in the original motor and in the motor with the optimized BIE for the same output torque are displayed in Fig. 10. The hot-spot (173°C) inside the slot of the original motor (i.e. without BIE) is located at the left hand side (i.e. centre of slot) as shown in Fig. 10 (a). For the motor with the optimized BIE the hotspot temperature is reduced down to 156°C, and the hotspot location is shifted to the centre of Fig. 10 (b) (i.e. to the mid-position of the half slot).

In light of the analysis performed, an optimized BIE width of 2.2 mm for a BIE depth 21.7 mm is identified as the optimal selection to pursue with for the experimental validation. The copper fill factor with the proposed motor

decreases by 11.28% from 0.4583 in the original motor to 0.4066, as shown in Fig. 4.

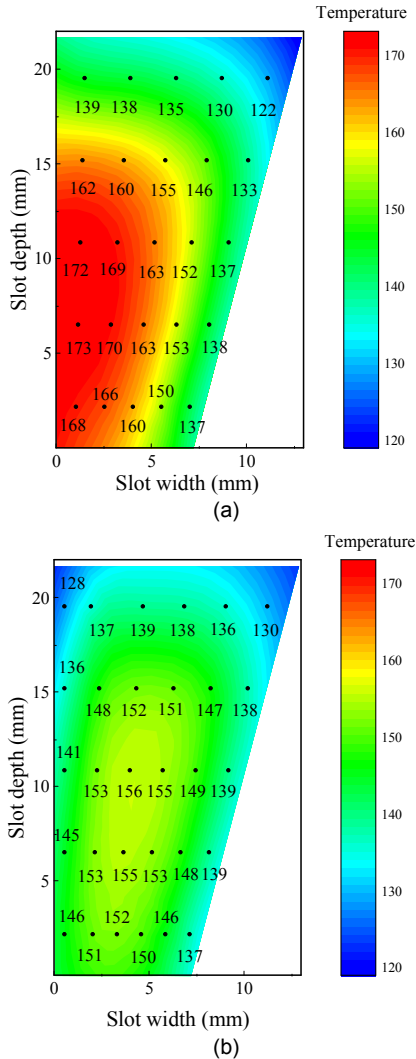


Fig. 10. Temperature contour (a) original motor. (b) motor with BIE

D. Generalization aspects

The previous sections have shown the benefit of the proposed BIE. To generalize the relationship of back-iron extension geometry with motor slot geometry with the aim of achieving the best thermal performance, a series of scaled motors based on the studied traction motor are analyzed. In this exercise the dimensions of the machine are scaled from 1/4th to 4 times the dimensions of the original motor. The ratio of the back-iron extension width ' s_1 ' to the slot bottom width ' s_2 ' is plotted versus the slot bottom width in Fig. 11, considering the back-iron extension depth ' d_1 ' to be always equal the slot depth ' d_2 '. From Fig. 11, it can be seen that the optimal ratio of ' s_1/s_2 ' increases in an almost linear relationship with the slot bottom width when the slot bottom width is small, increasing from 6.2 % to 11% when the slot width increases from 10mm to 21mm. As the slot bottom width increases beyond 40mm, the optimal ratio of ' s_1/s_2 ' flattens out to around 12-13%.

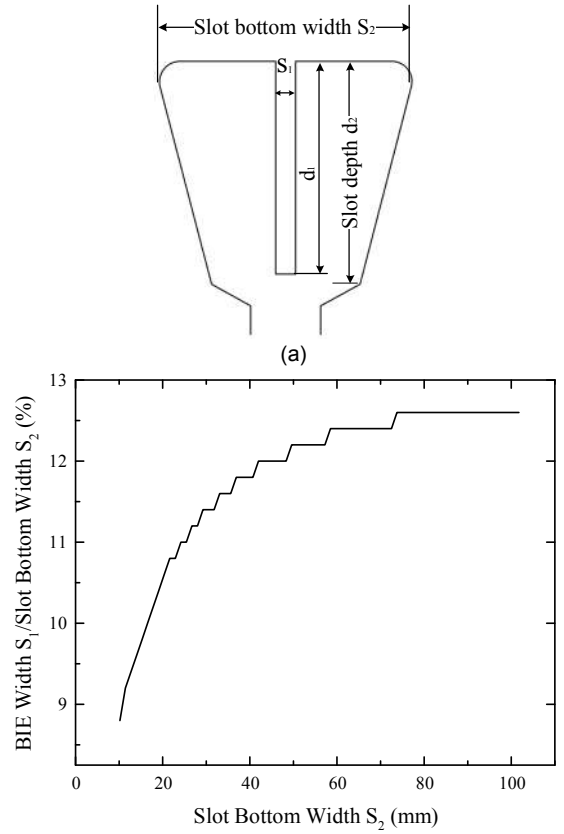


Fig. 11. Optimized back-iron extension geometry

III. EXPERIMENTAL VALIDATION

A. Experimental set up

Two stator segments with a water-cooled housing are designed and built purposely for the back-iron extension thermal benefit validation. One segment represents the original stator configuration, while the other segment features the optimized back-iron extension dimension. The segments are of the same length as with the original traction motor. Iron losses are neglected in the validation process as they are small compared to the copper losses generated in the slot. Therefore, to simplify the manufacturing procedure, both segments are made from solid steel.

As discussed in section II, the introduction of the back-iron extension in the slot reduces the slot area available for winding, thus resulting in a lower copper fill factor and higher copper losses. The number of strands per turn is thus reduced accordingly for the segment with the BIE.

A plurality of thermocouples (TCs) are placed in the manufactured segments to accurately characterize and compare the thermal performance. These are placed in the slot (TC1-TC4), end-winding and stator back-iron (TC5) as shown in Fig. 12. For the stator segment representing the original stator, there are three TCs in each slot, with TC3 placed in the location where the hotspot is expected. TC1 and TC2 are placed between the slot liner and the winding. On the other hand, in the segment with the back-iron extension, there are four TCs, and in this case TC4 corresponds to the location where the hotspot is expected. TC3, similarly to TC1 and TC2, is located between the winding and slot liner, which is used for ground insulation.

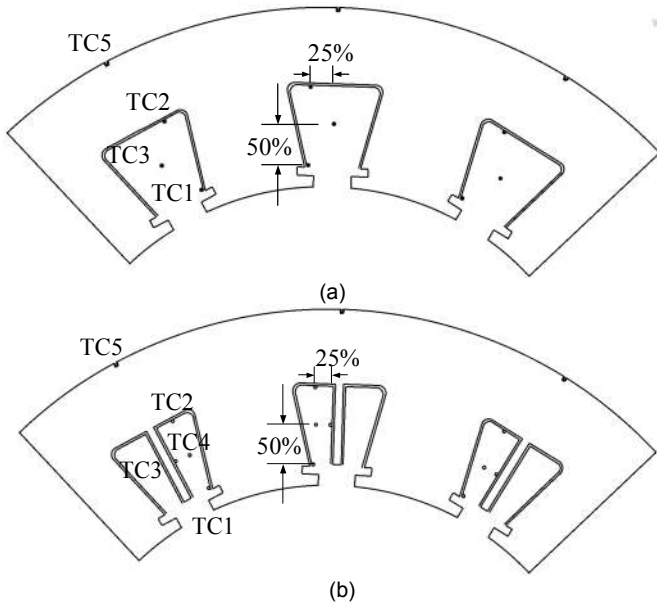


Fig. 12. Layout and thermocouple locations (a) original stator segment. (b) stator segment with back iron extension

The segments are fed by a DC current in order to generate heat in the windings. The segments are thermally insulated from air hence the heat generated in the segments can be considered as being transferred to the coolant in the housing and pumped out to the water chiller. The experimental setup is shown in Fig. 13, including the segment under test, DC power supply, temperature logger and water chiller.

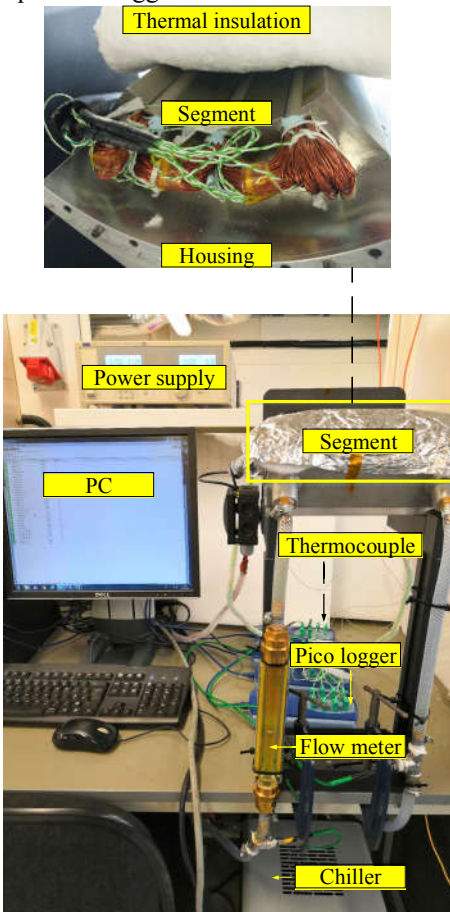


Fig. 13. Experimental setup

B. Thermal experiment results

As discussed in section II, the back-iron extension reduces the winding temperature by improving the problem of low equivalent thermal conductivity inside the slot. The equivalent thermal conductivity inside the slot affects the degree of thermal benefits the back-iron extension can bring. Varnish, the thermal conductivity of which is around 0.2 – 0.3 W/(mK), depending on the grade, plays an important role in determining the equivalent thermal conductivity inside the slot. Therefore, the two segments were varnished by vacuum pressure impregnation (VPI) which ensures a good fill quality and consistency by the impregnation resin.

Fig. 14 shows the power/losses as a function of the input current for the varnished segments. As shown in this figure, the power output from the power supply is higher than the heat generated in the segments, as there are losses in the connection wires and wire connection junctions between the power supply and the segments. Furthermore, from Fig. 14, it is evident that the decreased copper fill factor due to the space occupied by the back-iron extension results into a higher electrical resistance in the segment with BIE and thus results in a higher losses for the same current.

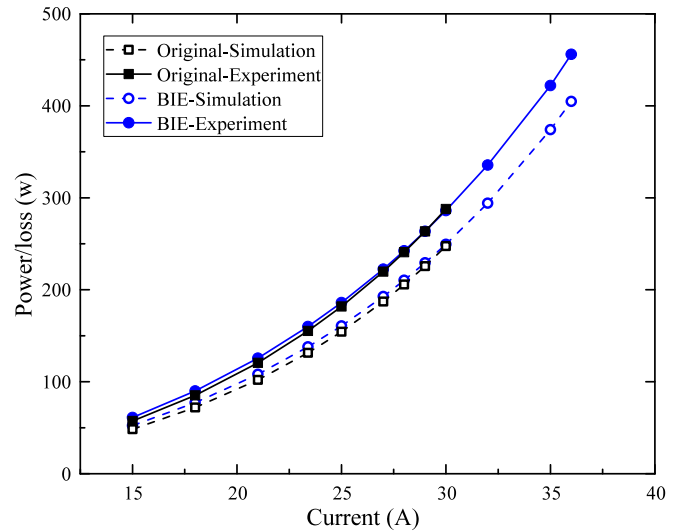


Fig. 14. Power comparison in the varnished segments

Fig. 15 shows the measured and predicted peak temperatures for the varnished segments as a function of the input current. The peak winding temperature as predicted in LPTN modelling and from the experimental results of each segment for different currents are plotted and compared. The experimental tests agree well with the predictions, with deviations which can be attributed to things such as manufacturing processes and precise TC placement.

From Fig. 15, as expected, it is noted that the peak temperature for both stator segments increases with current, however the rate of rise varies between the two, with the one featuring the BIE slowing down the rise and resulting into a lower increasing rate.

For the segment representing the original stator, an input current of 30A translates to a hotspot of 180°C, while for the

varnished BIE segment, for the same current the peak temperature is 132°C or around 26.7% lower.

Alternatively, for the same peak temperature of 180°C, the current in the varnished BIE segment can be increased from 30.4A (8.87 A/mm²) to 36.5A (11.71 A/mm²).

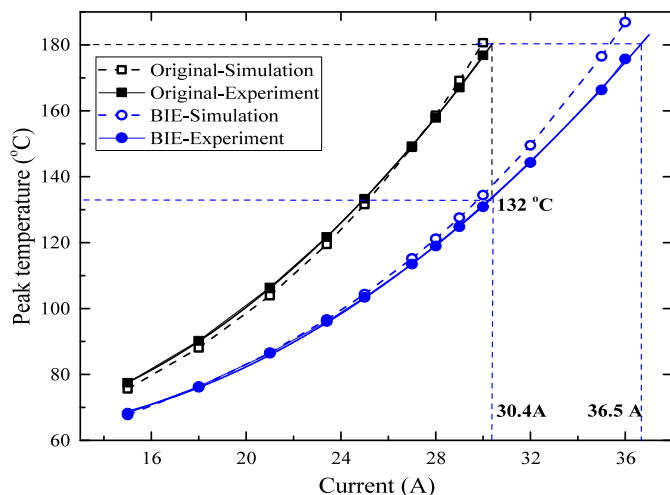


Fig. 15 Back-iron extension thermal benefits

Fig. 15 shows significant benefits resulting from the adaptation of BIE. It is worth noting that the BIE benefit is even more significant if the equivalent thermal conductivity in the slot is small, since the equivalent thermal resistance inside the slot occupies a large percentage of the total equivalent thermal resistance between hot spot and coolant.

IV. CONCLUSION

For next generation electrical machines with a step change in performance metrics, the improvement in thermal management is one of the most important enablers in pushing operational boundaries. Often improvements in thermal management are obtained at the cost of more intensive cooling, such as by flooding the stator or using costly high thermal conductivity materials. This paper proposes a simple, novel way to improve the motor thermal performance with concentrated winding by extending part of the back-iron in the slot, shortening the heat removal path between the hot spot in the slot and coolant. Such a modification is low-cost to implement as it doesn't involve any new additional material, and can be achieved by the appropriate design of the lamination punching tool in a motor volume manufacturing environment. It translates to marked thermal benefits, especially in electrical machines with wider slot, such as concentrated-wound machines. Moreover, it is also applicable to other types of machines and/or winding configurations. For single layer concentrated windings, where the coil section is usually thicker, the thermal benefit could be even more significant with respect to the double-layer case presented in this paper. For traditional distributed winding, implementing the proposed method needs careful consideration. The impact on the copper fill factor and end-winding length is significant. In addition any resulting benefit is likely to be limited as

distributed windings naturally have a higher number of slots per pole which reduces the issues with winding hotspots. Taking an existing electric vehicle traction motor, combined thermal and electromagnetic analysis of different back-iron extension geometries has been presented, and it has been experimentally shown that with the appropriate multi-domain optimization a significant 26.7 % peak winding temperature reduction can be achieved with the back-iron extension. The simplicity of the presented solution combined with its technical effectiveness make it a strongly enabling solution for next generation improved performance motors.

REFERENCES

- [1] D. Gerada, A. Mebarki, N. L. Brown, C. Gerada, A. Cavagnino, and A. Boglietti, "High-speed electrical machines: Technologies, trends, and developments," *IEEE Transactions on Industrial Electronics*, vol. 61, no. 6, pp. 2946-2959, 2014.
- [2] D. Golovanov, L. Papini, D. Gerada, Z. Xu, and C. Gerada, "Multidomain Optimization of High-Power-Density PM Electrical Machines for System Architecture Selection," *IEEE Transactions on Industrial Electronics*, vol. 65, no. 7, pp. 5302-5312, 2018.
- [3] N. Uzhegov, E. Kurvinen, J. Nerg, J. Pyrhönen, J. T. Sopenan, and S. Shirinskii, "Multidisciplinary design process of a 6-slot 2-pole high-speed permanent-magnet synchronous machine," *IEEE Transactions on Industrial Electronics*, vol. 63, no. 2, pp. 784-795, 2016.
- [4] A. Walker, M. Galea, D. Gerada, C. Gerada, A. Mebarki, and N. Brown, "Development and design of a high performance traction machine for the FreedomCar 2020 traction machine targets," in *Electrical Machines (ICEM), 2016 XXII International Conference on*, 2016, pp. 1611-1617: IEEE.
- [5] M. Galea, C. Gerada, T. Raminosa, and P. Wheeler, "A thermal improvement technique for the phase windings of electrical machines," *IEEE Transactions on Industry Applications*, vol. 48, no. 1, pp. 79-87, 2012.
- [6] A. L. Rocca, S. J. Pickering, C. Eastwick, and C. Gerada, "Enhanced cooling for an electric starter-generator for aerospace application," in *7th IET International Conference on Power Electronics, Machines and Drives (PEMD 2014)*, 2014, pp. 1-7.
- [7] Z. Xu *et al.*, "A semi-flooded cooling for a high speed machine: Concept, design and practice of an oil sleeve," in *Industrial Electronics Society, IECON 2017-43rd Annual Conference of the IEEE*, 2017, pp. 8557-8562: IEEE.
- [8] R. J. Wang and G. C. Heyns, "Thermal analysis of a water-cooled interior permanent magnet traction machine," in *2013 IEEE International Conference on Industrial Technology (ICIT)*, 2013, pp. 416-421.
- [9] P. Ponomarev, M. Polikarpova, and J. Pyrhönen, "Thermal modeling of directly-oil-cooled permanent magnet synchronous machine," in *2012 XXth International Conference on Electrical Machines*, 2012, pp. 1882-1887.
- [10] A. Boglietti, A. Cavagnino, M. Popescu, D. Staton, D. Hawkins, and J. Goss, "Modern heat extraction systems for power traction machines-a review," *IEEE Transactions on Industry Applications*, vol. 52, no. 3, pp. 2167-2175, 2016.
- [11] A. Boglietti, A. Cavagnino, D. Staton, M. Shanel, M. Mueller, and C. Mejuto, "Evolution and modern approaches for thermal analysis of electrical machines," *IEEE Transactions on industrial electronics*, vol. 56, no. 3, pp. 871-882, 2009.
- [12] M. Schiefer and M. Doppelbauer, "Indirect slot cooling for high-power-density machines with concentrated winding," in *2015 IEEE International Electric Machines & Drives Conference (IEMDC)*, 2015, pp. 1820-1825.
- [13] S. A. Semidey and J. R. Mayor, "Experimentation of an Electric Machine Technology Demonstrator Incorporating Direct Winding Heat Exchangers," *IEEE Trans. Industrial Electronics*, vol. 61, no. 10, pp. 5771-5778, 2014.
- [14] A. Reinap *et al.*, "Electrical machine design with directly cooled laminated fractional pitch windings," in *5th International Electric Drives Production Conference (E) DPC*, 2015.
- [15] C. Tighe, C. Gerada, and S. Pickering, "Assessment of cooling methods for increased power density in electrical machines," in *2016 XXII*

- International Conference on Electrical Machines (ICEM)*, 2016, pp. 2626-2632.
- [16] P. Lindh *et al.*, "Direct liquid cooling method verified with an axial-flux permanent-magnet traction machine prototype," *IEEE Transactions on Industrial Electronics*, vol. 64, no. 8, pp. 6086-6095, 2017.
- [17] M. Polikarpova, S. Semken, and J. Pyrhönen, "Reliability analysis of a direct-liquid cooling system of direct drive permanent magnet synchronous generator," in *Reliability and Maintainability Symposium (RAMS), 2013 Proceedings-Annual*, 2013, pp. 1-6: IEEE.
- [18] P. Mellor, R. Wrobel, A. Mlot, T. Horseman, and D. Staton, "Influence of winding design on losses in brushless AC IPM propulsion motors," in *Energy Conversion Congress and Exposition (ECCE), 2011 IEEE*, 2011, pp. 2782-2789: IEEE.
- [19] A. Nollau and D. Gerling, "Novel cooling methods using flux-barriers," in *Electrical Machines (ICEM), 2014 International Conference on*, 2014, pp. 1328-1333: IEEE.
- [20] R. Wrobel, S. J. Williamson, N. Simpson, S. Ayat, J. Yon, and P. H. Mellor, "Impact of slot shape on loss and thermal behaviour of open-slot modular stator windings," in *Energy Conversion Congress and Exposition (ECCE), 2015 IEEE*, 2015, pp. 4433-4440: IEEE.
- [21] D. Staton, A. Boglietti, and A. Cavagnino, "Solving the more difficult aspects of electric motor thermal analysis in small and medium size industrial induction motors," *IEEE Transactions on Energy Conversion*, vol. 20, no. 3, pp. 620-628, 2005.
- [22] A. Boglietti, M. Cossale, S. Vaschetto, and T. Dutra, "Thermal conductivity evaluation of fractional-slot concentrated-winding machines," *IEEE Transactions on Industry Applications*, vol. 53, no. 3, pp. 2059-2065, 2017.
- [23] S. Nategh, Z. Huang, A. Krings, O. Wallmark, and M. Leksell, "Thermal modeling of directly cooled electric machines using lumped parameter and limited CFD analysis," *IEEE Transactions on Energy Conversion*, vol. 28, no. 4, pp. 979-990, 2013.
- [24] R. Wrobel and P. Mellor, "A general cuboidal element for three-dimensional thermal modelling," *IEEE Transactions on Magnetics*, vol. 46, no. 8, pp. 3197-3200, 2010.
- [25] P. Mellor, D. Roberts, and D. Turner, "Lumped parameter thermal model for electrical machines of TEFC design," in *IEE Proceedings B-Electric Power Applications*, 1991, vol. 138, no. 5, pp. 205-218: IET.
- [26] V. Gnielinski, "New equations for heat and mass transfer in turbulent pipe and channel flow," *Int. Chem. Eng.*, vol. 16, no. 2, pp. 359-368, 1976.



Fengyu Zhang received B.E degree in thermal engineering from Huazhong University of Science and Technology, Wuhan, China in 2014. She is currently pursuing a Ph.D degree at University of Nottingham with a focus on thermal management of electrical machines. Her main research interests include high performance motors for transport applications and their multi-domain optimization.



David Gerada received the Ph.D. degree in high-speed electrical machines from University of Nottingham, Nottingham, U.K., in 2012.

From 2007 to 2016, he was with the R&D Department at Cummins, Stamford, U.K., first as an Electromagnetic Design Engineer (2007–2012), and then as a Senior Electromagnetic Design Engineer and Innovation Leader (2012–2016). At Cummins, he pioneered the design and development of high-speed electrical machines, transforming a challenging technology into a reliable one suitable for the transportation market, while establishing industry-wide-used metrics for such machinery. In 2016, he joined the University of Nottingham as a Senior Fellow in electrical machines, responsible for developing state-of-the-art electrical machines for future transportation which push existing technology boundaries, while propelling the new technologies to higher technology readiness levels.

Dr. Gerada is a Chartered Engineer in the U.K. and a member of the Institution of Engineering and Technology.



Zeyuan Xu received the Ph.D. degree in mechanical engineering from the University of Manchester, Manchester, U.K., in 2002.

He subsequently worked as a Research Fellow at UMIST, Brunel University, and the University of Nottingham. He is currently a Senior Research Fellow in thermo-mechanical design of high speed electrical machines within the PEMC group at the University of Nottingham, Nottingham, U.K. His main research interests include turbulent thermo-fluid flow, heat transfer enhancement, and thermal management of advanced electrical machines and power electronics.



Xiaochen Zhang (S'09-M'12) graduated from Harbin University of Science and Technology and received Master's Degree in 2006. He graduated from Harbin Institute of Electrical Technology and received Doctor's Degree in 2012.

He is with the Department of Electric and Electronic Engineering, The University of Nottingham, Nottingham, UK. His research interests include research on electromagnetic and thermal analysis on electrical machine, especially in permanent magnetic machines and high speed

machines.



Chris Tighe received the MEng and Ph.D. degrees in mechanical engineering from the University of Nottingham, U.K., in 2007 and 2011, respectively. After graduating, he spent time working in the electrical generator industry and in various research and commercial machine development positions at the University of Nottingham. He is now the proprietor of Electrical Cooling Solutions, an engineering design consultancy specialising in the thermal management of electrical machines and power electronics.



He Zhang received his B.Eng. degree from Zhejiang University, China, in 2002. He obtained the MSc. and Ph.D. degree in electrical machines from The University of Nottingham, UK, in 2004 and 2009 respectively. After this he worked as Research Fellow at the University and Director of BestMotion Technology Centre. He moved to University of Nottingham Ningbo China as Senior Research Fellow in 2014 and Principal Research Fellow in 2016. Currently he is the Director of Nottingham Electrification Centre (NEC) within the Power electronics, Machines and Control research group in University Of Nottingham. His research interests include high performance electric machines and drives for transport electrification.



Chris Gerada (M'05-SM'12) received the Ph.D. degree in numerical modelling of electrical machines from The University of Nottingham, Nottingham, U.K., in 2005.

He subsequently worked as a Researcher with The University of Nottingham on high-performance electrical drives and on the design and modelling of electromagnetic actuators for aerospace applications. In 2008, he was appointed as a Lecturer in electrical machines; in 2011, as an Associate Professor; and in 2013, as a Professor at The University of Nottingham. He was awarded a Research Chair from the Royal Academy of Engineering in 2013 and his main research interests include the design and modelling of high-performance electric drives and machines.

Prof. Gerada serves as an Associate Editor for the IEEE TRANSACTIONS ON INDUSTRY APPLICATIONS and is the past Chair of the IEEE IES Electrical Machines Committee.